Dynamic Windowing Algorithm for the Fast and Accurate Determination of Luminescence Lifetimes

ARTICLE *in* ANALYTICAL CHEMISTRY · APRIL 2012

Impact Factor: 5.64 · DOI: 10.1021/ac300023q · Source: PubMed

2 AUTHORS:

Bradley Bruce Collier
Northeastern University
12 PUBLICATIONS **43** CITATIONS

SEE PROFILE

Michael J McShane
Texas A&M University
180 PUBLICATIONS **3,309** CITATIONS

SEE PROFILE

analytical chemistry

Article

pubs.acs.org/ac

Dynamic Windowing Algorithm for the Fast and Accurate Determination of Luminescence Lifetimes

Bradley B. Collier[†] and Michael J. McShane*[,†,‡]

[†]Department of Biomedical Engineering and [‡]Materials Science and Engineering Program, Texas A&M University, College Station, Texas 77843, United States

ABSTRACT: An algorithm for the accurate calculation of luminescence lifetimes in near-real-time is described. The dynamic rapid lifetime determination (DRLD) method uses a window-summing technique and dynamically selects the appropriate window width for each lifetime decay such that a large range of lifetimes can be accurately calculated. The selection of window width is based on an optimal range of window-sum ratios. The algorithm was compared to alternative approaches for rapid lifetime determination as well as nonlinear least-squares (NLLS) fitting in both simulated and real experimental conditions. A palladium porphyrin was used as a model luminophore to quantitatively evaluate the algorithm in a dynamic situation, where oxygen concentration was modulated to induce a change in lifetime. Unlike other window-summing techniques, the new algorithm calculates lifetimes that are not significantly different than the slower, traditional NLLS. In addition, the computation time required to calculate the lifetime is 4 orders of magnitude less than NLLS and 2 orders less than other iterative methods. This advance will improve the accuracy of real-time measurements that must be made on samples that are expected to exhibit widely varying lifetimes, such as sensors and biosensors.

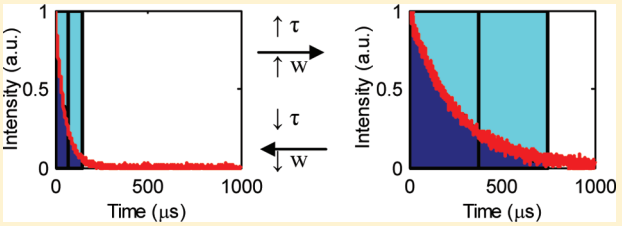

Luminescent sensing and characterization have become widely researched areas in biomedical, environmental, and food industries because of their ability to provide greater sensitivity and measurement flexibility when compared to electrochemical analysis schemes.[1,2] In the past, intensity measurements have been predominantly used to measure analyte concentrations or physical properties; however, these methods are susceptible to many sources of error including photobleaching, drift in light source intensity, and variations in dye concentrations from sensor to sensor.[3−5] These issues can be overcome by measuring the rate of luminescence decay or "lifetime" which is independent of the intensity.[6,7]

Although lifetime measurements can be made using either time-domain or frequency-domain techniques, the former can be advantageous because of its ability to easily eliminate scattering and shorter lifetime fluorescence from calculations. For example, many proteins found in the body, including collagen and elastin, are known to emit nanosecond lifetimes which can effect lifetime calculations of the dye. In addition, time-domain methods have been shown to have a higher precision than frequency-domain methods especially at lower intensities.[7,8] Traditionally, linear and nonlinear least-squares fittings have been used to determine the lifetime during time-domain measurements, but these methods require extensive computing power due to the large number of iterations required to arrive at an accurate estimate. The lifetimes calculated with fittings are also dependent on the initial guesses for each parameter.[9] If the initial guesses are not relatively close to the true values, convergence of the fit will take more time. A complex fit can also lead to the selection of the fit parameters at their local minima leading to biased estimates.[9]

To collect exponentially decaying data which exhibit a rate of change that varies dramatically during the decay period, investigators previously utilized logarithmic sample rates to reduce the number of data points recorded and effectively average out noise in the signal.[10−12] Although these methods were developed to optimize data collection and minimize storage, advances in computer technology have yielded virtually limitless capacity. However, several groups have also investigated alternative processing techniques using gate- or window-sums to calculate lifetimes as a way to enhance calculation speed for real-time analysis.[13−18] The rapid lifetime determination (RLD) method utilizes two windows of equal width applied over the decay of a luminophore.[15] By summing over the width of the window, the lifetime can be determined using:

$$\tau = \frac{\Delta t}{\ln(W_1/W_2)} \quad (1)$$

where Δt is the window width and W_1 and W_2 are the sums for windows 1 and 2, respectively (Figure 1). This calculation is much faster than the traditional fitting methods but can still be susceptible to errors which occur because a single static window width is oftentimes not optimal for lifetimes much shorter or longer than the widths.[4,14−17] For example, this becomes especially problematic for sensing applications where dynamic lifetimes of a wide range are utilized. In order to overcome this problem, several methods have been developed in order to

Received: January 3, 2012
Accepted: April 17, 2012
Published: April 17, 2012

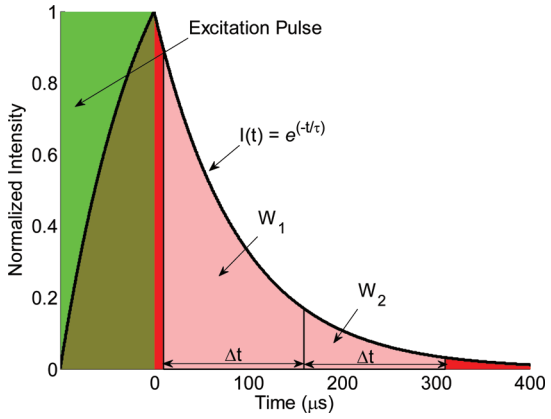

Figure 1. Diagram of the basic RLD lifetime determination approach with contiguous windows of equal width.

appropriately select the window width and increase the accuracy of lifetime calculations. These methods maintain the advantage of speed over nonlinear least-squares (NLLS) but are still limited in range because of the static window width.[14−18]

The original two window-based method, referred to here as the contiguous RLD (CRLD) method, utilizes windows of equal width run back-to-back to calculate the lifetime.[15] The second window of the overlapping RLD (ORLD) method, however, begins before the first one ends.[17] Both of these methods utilize eq 1 to calculate the lifetime. However, the generalized RLD (GRLD) method, utilizes overlapping windows of different width which requires a different equation to calculate lifetime.[18]

For the current work, a computer-based algorithm to dynamically determine the appropriate window width was evaluated as a way to increase the accuracy of lifetime calculations compared to those methods with a static window width. In practice, this method will only be limited by the sampling frequency and the number of data points recorded over time, but in theory this method could calculate the lifetime of any response. As with NLLS, however, a larger range of possible lifetimes will lead to an increased number of iterations performed and increased computation time. This approach is based on the original two-window RLD where the windows are contiguous and of equal width but will be applicable to a much more extensive range because the window widths are allowed to change dynamically as the lifetime changes.

THEORY

The optimal window width for lifetime determination is usually described by the ratio of the window width, Δt, to the lifetime, τ.[14,15,17,18] Ballew and Demas initially proposed an optimal ratio for contiguous RLD near $\Delta t/\tau = 2.5$ and other groups later describe an optimal region from 1 to 3 $\Delta t/\tau$.[15,17,18] To implement dynamic rapid lifetime determination (DRLD), the ratio of window-sums can be correlated to $\Delta t/\tau$ by rearranging eq 1:

$$W = \frac{W_1}{W_2} = e^{\frac{\Delta t}{\tau}} \tag{2}$$

where W is the ratio of the window-sums. The optimal range for $\Delta t/\tau$ can then be plugged into this equation to get the corresponding optimal range for W. When performing the calculation for data that exhibit significant changes in τ, the window widths should be adjusted for every lifetime calculation until W is within the optimal range or another termination condition is met.

To implement a dynamic window change, the window width can be adjusted by multiplying the previously calculated lifetime by a value that lies in the middle of the chosen optimal range of $\Delta t/\tau$. The window size is initially set to a small value so that a maximum window change is only used for increases in window width. Maximum window widths and maximum window changes are also implemented to prevent programming errors. Protection from negative W values, which can occur when the decay shows low signal-to-noise ratio, should also be implemented in this algorithm. The lifetime is recalculated until W is in the optimal range, the maximum width is reached, or a maximum number of loops has been reached. A flow-chart of the entire algorithm can be seen in Figure 2. In this work, we describe the implementation of this algorithm in a hardware and software system and demonstrate the function in a series of experiments.

MATERIALS AND METHODS

Lifetime Techniques. In addition to DRLD and NLLS, the three other static windowing methods described previously were used for comparison of lifetime calculations. The width of the windows for CRLD was set to $0.25\overline{\tau}$ which was previously

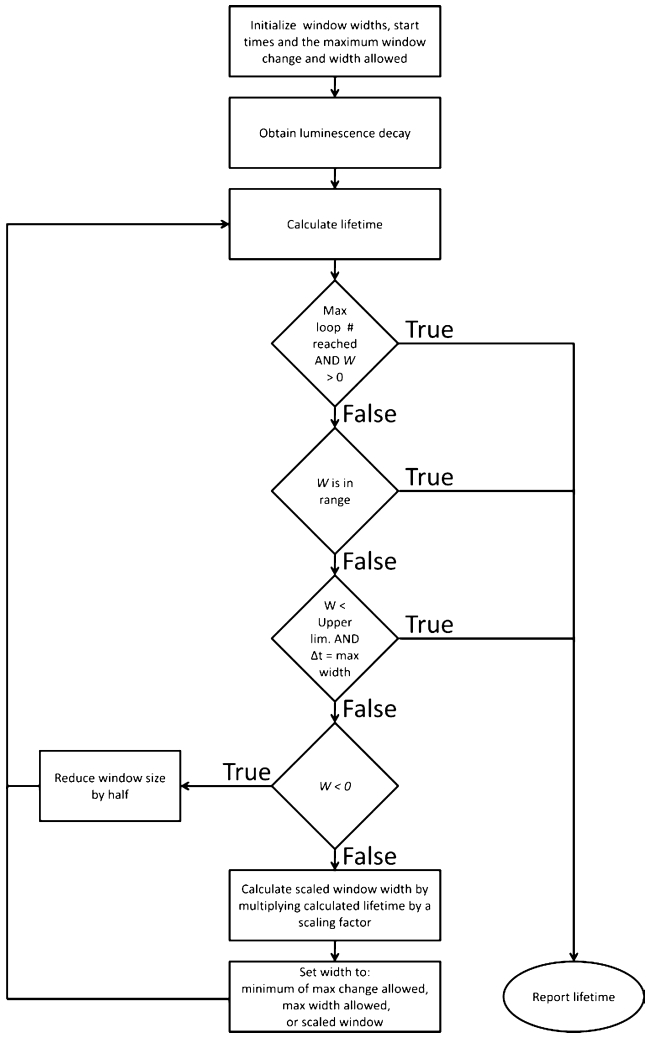

Figure 2. Flowchart of dynamic windowing algorithm operation.

dx.doi.org/10.1021/ac300023q | Anal. Chem. 2012, 84, 4725−4731

determined to be the optimal width for this method where $\bar{\tau}$ is the mean expected lifetime.[16] Two variations of the ORLD method were utilized to calculate the lifetime. Both utilize a second window start time of $0.25\bar{\tau}$, but the window widths were to set to $0.5\bar{\tau}$ and $1\bar{\tau}$ for ORLD1 and ORLD2, respectively. For GRLD, the equation below was adapted from the original equation to incorporate an initial delay of the window start times:

$$\frac{W_2}{W_1} = \frac{e^{-Q(X+Y+P)} - e^{-Q(X+Y)}}{e^{-Q(X+1)} - e^{-QX}} \quad (3)$$

where X is the fractional delay of W_1 in terms of Δt, Y is the fractional delay of W_2 (relative to W_1) in terms of Δt, and P is the width of W_2 in multiples of Δt. For this work, Y and P were set to 0.25 and 12, respectively, as specified in the literature.[18] Using an iterative solver, Q is solved for and then plugged into

$$\tau = \frac{\Delta t}{Q} \quad (4)$$

to obtain a lifetime. The width of W_1 or Δt was set to $0.25\bar{\tau}$ because an optimal value was not previously determined. Other iterative window-summing methods for lifetime calculations are available but often require 10 or more windows. This number of windows means greater complexity and increased computation. These methods will not be compared here but have been elsewhere.[19−21] For calculations performed, an initial delay of window start times was set to 0.8 μs in order to eliminate backscattered excitation light from the lifetime calculations. This delay represents a single data point collected for each decay (based on the sampling rate) and will not affect lifetime calculations or optimal window widths. Theoretical implementation of each of these methods can be seen in Figure 3.

Modeled Lifetime Responses. Initial modeling investigated the possible calculation errors in static window width methods. If a dynamic windowing algorithm is not used and the lifetime response changes dramatically, a large error may be observed. From our calculations, if the lifetime response was 25 μs and the windows were 37.6 μs ($\Delta t/\tau$ = 1.5), the calculated lifetimes would have a very good accuracy and repeatability as indicated by a mean modeled lifetime calculation of 24.8 μs and a standard deviation of 0.322 μs (n = 10, SNR = 10). However, if the lifetimes were to suddenly change to 250 μs, the precision of the measurement is greatly reduced as seen by modeled calculations with a mean lifetime of 264.2 μs and a standard deviation of 39.2 μs (n = 10, SNR = 10).

To test the algorithm described above, a lifetime profile was designed in MATLAB (Mathworks) to simulate a real-time response and test the ability of different window-summing lifetime calculation methods to calculate a range of lifetimes. A decay for each lifetime was simulated with a SNR of 10 (Figure 4), and each of the five methods were used to calculate τ. The residuals and R^2 values for each method were also calculated to determine the accuracy of each method.

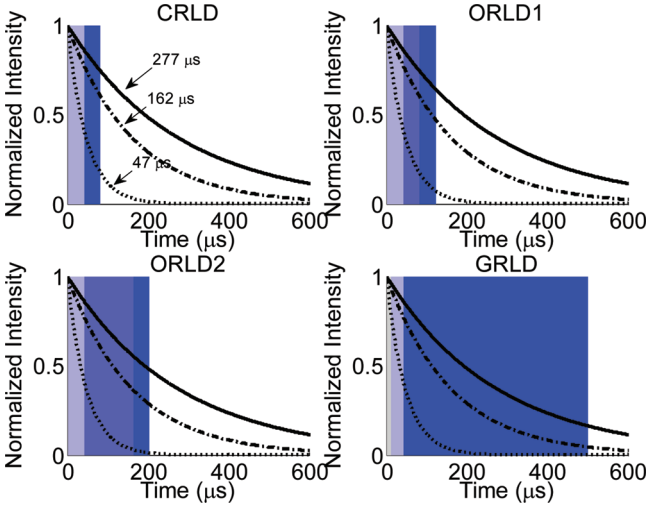

Figure 3. Theoretical implementation over three different lifetimes of the four static window methods utilized to compare to DRLD. W_1 is represented by a light colored box and W_2 is represented by a dark colored box. Any overlap of the windows is represented by a shade in between the two window colors.

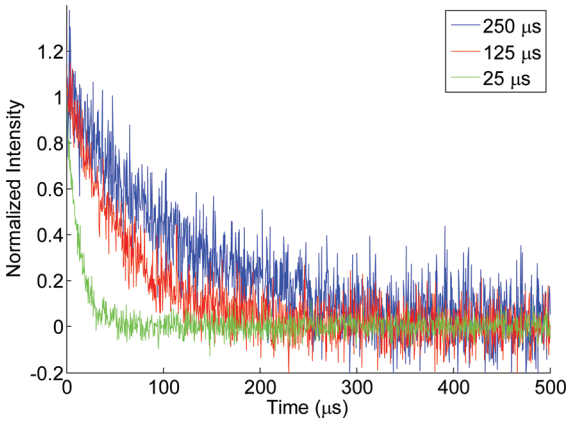

Figure 4. Examples of modeled luminescence decays with an SNR of 10.

Custom Lifetime Measurement System. A custom time-domain lifetime measurement system was developed to experimentally demonstrate the DRLD technique. For luminophore excitation, a fiber optic green LED (530 nm peak, Industrial Fiber Optics, Tempe, AZ) was utilized with a driver circuit (see Figure 5) to improve the operating speed (ns rise and fall times) of the diode. The circuit consisted of a transistor and resistors and capacitors. Luminescence detection was performed using an avalanche photodiode module (APD, C5460, Hamamatsu). Two plano-convex lenses (LA1951-A, Thor Laboratories) were used to collect the luminescence from a bifurcated fiber bundle and focus it onto the active area of the

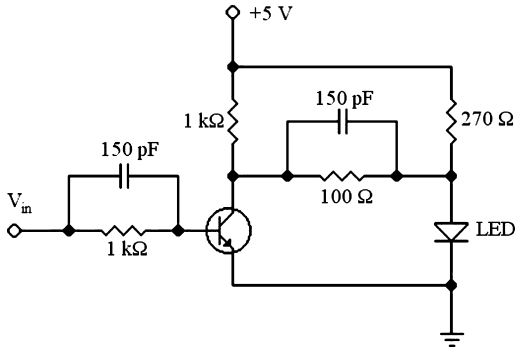

Figure 5. Circuit used to drive LED excitation where V_{in} is the control voltage.

dx.doi.org/10.1021/ac300023q | Anal. Chem. 2012, 84, 4725−4731

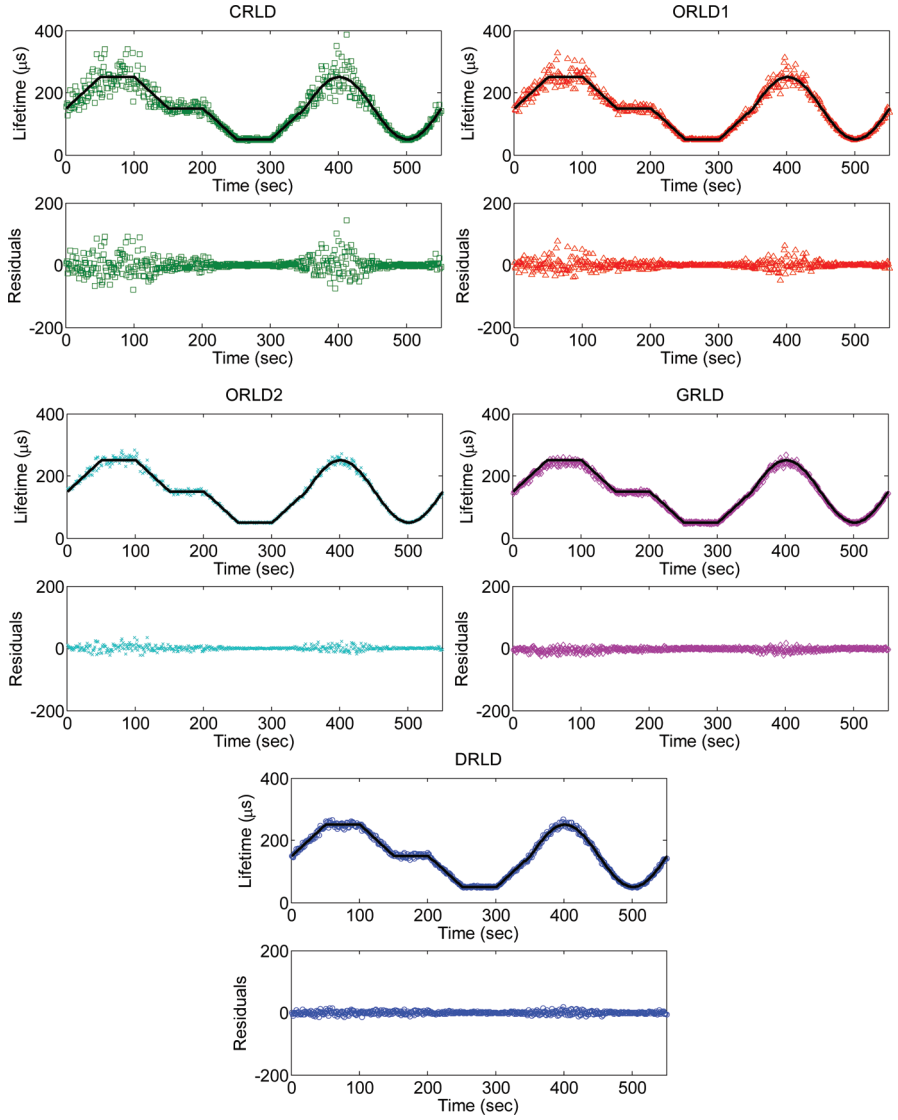

Figure 6. The lifetimes calculated for each window-sum based method in response to a simulated profile can be found in the top portion of each graph while the residuals of those calculations can be found on the bottom. The black line represents the simulated lifetime for each point in time.

APD. A long-pass filter (3RD620LP, Omega Optical) was also used to reduce interference from backscattered excitation light. A data acquisition board (USB-6259, National Instruments) was used to provide an excitation signal to the LED and collect the emission signal with a sampling rate of 1.25 MHz. Custom control programs were also developed using LabVIEW development software (National Instruments). A diagram of the system and its components can be found in a previous publication.[22]

During dynamic response testing and decay collection, a 40 Hz rectangular excitation signal was used to excite the luminophore and 40 raw decays were summed to yield one decay for lifetime calculations. A background signal was also collected at 40 Hz for 1 s before each excitation and subtracted out of the summed decay. A total of 25 summed decays were obtained for each steady-state response. The summed decays with background subtracted out will henceforth be referred to only as decays.

To implement DRLD, the initial window width was set to 10 μs and the maximum number of loops was set to 10. The maximum window change allowed for one loop was set to 50 μs, and the maximum window width allowed was set based on the 1000 μs total acquisition time. The windows were also delayed 0.8 μs from the end of the excitation pulse in order to reduce error from backscattered excitation light. Most importantly, the range of $\Delta t/\tau$ was chosen to be from 1 to 2, giving W the corresponding range of 2.7 to 7.4.

In Vitro Testing and Comparison. Oxygen sensors were exposed to six different oxygen concentrations in random order during testing. Although real-time calculations were obtained using the proposed dynamic windowing algorithm (data not shown), 25 luminescence decays for each oxygen concentration were also saved for postprocessing to compare the accuracy and computation time required for the various methods. As a standard for comparison, lifetimes were calculated with a monoexponential fit using a nonlinear least-squares (NLLS) solver. These lifetimes were determined first and utilized to determine $\overline{\tau}$ by averaging the lifetime at the minimum and maximum concentrations measured. This value was used for other lifetime calculation methods to determine the appropriate window width. Mean R^2 values were obtained for the fittings at each oxygen concentration. The SNR at each concentration was

dx.doi.org/10.1021/ac300023q | *Anal. Chem.* 2012, 84, 4725−4731

also determined by dividing the mean NLLS lifetime by the standard deviation. The NLLS values were considered as the archetype lifetime measurements and were used to determine the accuracy of the other methods. Programs for each different lifetime calculation were written using MATLAB and computation time of each lifetime calculation was determined using the "tic" and "toc" functions.

Oxygen Sensors and in Vitro Experimental Setup. Porous, amine-modified silica microspheres (YMC America, Inc., 10.3 μm average diameter, 13.1 nm average pore diameter) were used as the sensor matrix. Palladium(II) meso-Tetra(4-carboxyphenyl) porphine (PdP, 710 nm peak emission) from Frontier Scientific was utilized as an oxygen-sensitive luminophore to create oxygen sensors by covalently coupling to the silica microspheres using a procedure described elsewhere.[23] The particles were then immobilized on a glass slide for testing. Two mass flow controllers and a controller (1179A and PR4000, MKS Instruments) were used to mix nitrogen and compressed air as a means to control dissolved oxygen concentration in the phosphate buffered saline solution which was used to perfuse oxygen sensors and validate the response. An amperometric oxygen sensor was also used to monitor the dissolved oxygen concentration (PA2000, Unisense). A peristaltic pump (Masterflex 7550-50, Cole Parmer) was used to deliver the buffer solution to the sensors.

RESULTS AND DISCUSSION

From the simulated response profile (Figure 6), all of the methods appear to be very accurate at low oxygen concentrations: that is when the windows are able to cover most of the decay. However, at higher oxygen concentrations, DRLD and GRLD were the only methods to keep a high accuracy, as indicated by the high R^2 values (>0.99) for both methods (Table 1). The decrease in accuracy at higher lifetimes is a result of the large amount of neglected data, as suggested by Figure 3. The original window-sums technique, CRLD, had the worst accuracy out of all of the methods and reinforces the limitation of fixed window widths. This initial testing suggested that DRLD would be able to perform well under dynamic testing conditions.

Table 1. Calculated R^2 Values for the Simulated Profile

method	R^2 for simulated profile
NLLS	
DRLD	0.996
CRLD	0.888
ORLD1	0.966
ORLD2	0.989
GRLD	0.992

The results from simulations that tested the effects of SNR can be found in Table 2. As expected, increasing the SNR leads to a decrease in the variability for each window-sum lifetime calculation method. However, as suggested by the results in Figure 6, this does not mean that the accuracy of the calculation increases. For example, the GRLD calculations for the 250 μs decay were not within one standard deviation of the actual lifetime for any SNR. The DRLD method, however, was always within one standard deviation of the actual lifetime and showed variability that was the same order of magnitude or less than the other methods. The variability for higher lifetime values was generally less than the other window sum methods with equal window width and more accurate than the GRLD method. This suggests that the DRLD method is better suited to determine the lifetime response for a range of values.

Table 2. Lifetimes Calculated Using Different Window-Summing Techniques for Simulated Decays with Different SNR[a]

lifetime (μs)	SNR	CRLD	ORLD1	ORLD2	GRLD	DRLD
50	5	49.89 (2.52)	48.58 (1.90)	50.06 (1.68)	49.00 (3.17)	50.61 (2.83)
	10	50.65 (1.79)	50.31 (0.97)	49.64 (1.15)	49.84 (1.15)	50.16 (1.56)
	20	50.05 (0.65)	50.05 (0.47)	49.85 (0.27)	49.04 (0.49)	49.93 (0.45)
150	5	151.75 (14.69)	150.3 (13.24)	145.88 (5.07)	144.72 (5.33)	148.09 (6.24)
	10	143.55 (13.39)	152.49 (7.8)	149.98 (4.56)	146.34 (3.93)	148.89 (4.9)
	20	150.91 (3.74)	150.07 (2.74)	150.69 (0.98)	147.00 (1.02)	149.50 (1.12)
250	5	305.99 (119.69)	238.65 (44.99)	241.85 (16.66)	238.64 (6.49)	253.52 (8.7)
	10	263.71 (56.80)	260.81 (36.11)	257.05 (13.25)	241.24 (8.81)	246.99 (7.61)
	20	257.01 (13.51)	252.7 (7.14)	251.61 (5.34)	241.70 (1.96)	249.99 (2.64)

[a]Values in parentheses represent one standard deviation for n = 10.

Using decays experimentally obtained using the custom lifetime measurement system (Figure 7), the lifetimes were calculated for each method and plotted for comparison (Table 3, Figure 8). It appears that the lifetimes calculated from the real-time decay data follow the trends observed from to the simulated profiles. The NLLS calculations did not have very high R^2 values at higher oxygen concentrations due to increased quenching of the dye's luminescence intensity which lead to a lower SNR (Table 3). From these fittings, $\bar{\tau}$ was found to be 162 μs. When comparing the window-summing techniques, DRLD showed a much higher accuracy than the other methods and was not significantly different than NLLS lifetimes (α = 0.05). The other methods tended to underestimate the lifetimes at lower oxygen concentrations. GRLD did not show the high

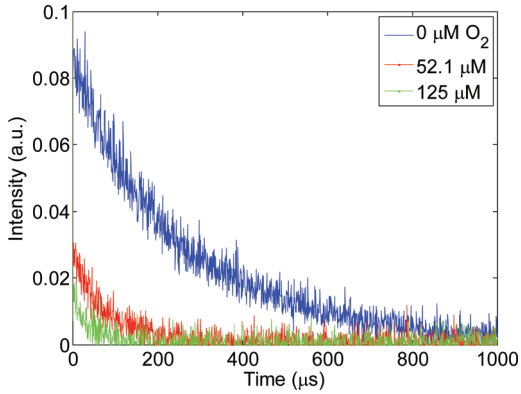

Figure 7. Example decays obtained from the custom lifetime measurement system for each oxygen concentration tested.

dx.doi.org/10.1021/ac300023q | Anal. Chem. 2012, 84, 4725−4731

Table 3. R^2 Values for NLLS Exponential Fittings of Lifetime Decays and Calculated SNR at Each Concentration[a]

				percent difference from NLLS				
oxygen concentration (μM)	R^2	SNR	NLLS lifetime (μs)	DRLD	CRLD	ORLD1	ORLD2	GRLD
0	0.969	43.2	277.07	0.680	−15.4	−13.5	−11.8	−10.0
27.3	0.885	22.6	117.28	2.50	−10.6	−8.61	−4.68	−2.43
52.1	0.780	15.7	91.48	0.295	−13.0	−9.30	−4.87	−0.420
76.4	0.562	8.95	62.24	8.21	−3.77	−1.44	5.65	5.42
101	0.505	6.45	58.45	1.49	−8.47	−2.35	2.13	2.34
125	0.334	5.24	46.84	2.13	−1.56	−1.73	2.89	−5.38

[a]Percent difference from NLLS for the different window-summing methods is also shown for each oxygen concentration.

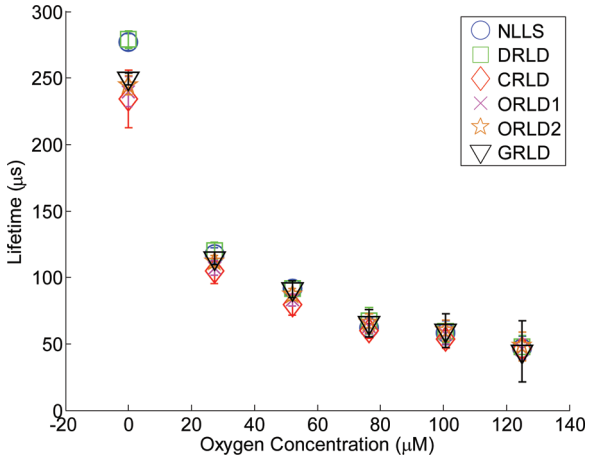

Figure 8. Lifetime response profile of the different window-sum methods compared to the lifetime calculated using traditional fittings. Error bars represent 95% confidence interval with n = 25.

level of accuracy expected, especially at 0 μM oxygen, and the confidence intervals (uncertainty) increased with oxygen concentration. Neither of these observations agrees with modeling results. The high mean R^2 value for the NLLS calculation at 0 μM suggests that the fitting calculation is correct and the decrease with increasing oxygen levels is most likely due to low SNR from the decays obtained. It is important to appreciate that the accuracy of all static window methods is expected to decrease for a larger range of oxygen values. Although larger windows can be utilized for GRLD to increase accuracy at lower concentrations, it would most likely result in decreased accuracy at higher concentrations. The accuracy of DRLD will most likely increase further with a decrease in the optimal range of W, but this could lead to an increase in computation time.

Following investigation of lifetime accuracy, the mean computation time was determined for the same set of data (Table 4). As expected, the noniterative methods were found to be much faster than the iterative methods. The speed of DRLD, CRLD, and ORLD is 2 orders of magnitude greater than GRLD and 4 orders greater than NLLS. This lifetime calculation speed will allow these window-summing techniques to overcome their reduced accuracy by making more measurements in the same period of time.[15] For example, with high speed excitation and collection, it could be possible to make over 100 DRLD lifetime measurements in the time it takes to make 1 NLLS measurement.

The speed and accuracy of DRLD has been shown capable of measuring a wide range of lifetimes for a common oxygen sensing system. These calculations displayed a high degree of accuracy and precision over a variety of oxygen concentrations. The DRLD technique can be easily implemented with a wide variety of current and future sensor technologies for analyte measurement.

Table 4. Real-Time Computation Data for Each Window-Based Lifetime Measurement Technique[a]

method	mean computation time (ms)
NLLS	307 (65.6)
DRLD	0.197 (0.043)
CRLD	0.143 (0.045)
ORLD1	0.137 (0.010)
ORLD2	0.149 (0.055)
GRLD	13.6 (0.200)

[a]Values in parentheses represent standard deviation with n = 25.

CONCLUSIONS

Our findings reveal that DRLD is more accurate than other window-summing lifetime calculation techniques with fixed window sizes when a wide range of lifetime values were considered. For the static window-summing methods, it is necessary to know beforehand the average expected lifetime to make accurate lifetime predictions. In contrast, DRLD is always accurate because it adjusts the window size and, despite this iterative approach, it is still more than one thousand times faster than traditional NLLS calculations. It is noteworthy that this algorithm may also be used with charge-coupled device (CCD) detectors with the window change not occurring until the next lifetime measurement. This dynamic windowing algorithm can be implemented with additional degrees of freedom, such as with overlapping windows in order to increase the optimal range of $\Delta t/\tau$[17] or with a three-window-sum calculation which does not require the background signal to be measured beforehand.[14] With the aid of current microprocessor technology, it is anticipated that this method can be utilized within numerous sensing applications to enable accurate dynamic lifetime predictions using low-cost mobile devices.

AUTHOR INFORMATION

Corresponding Author

*E-mail: mcshane@tamu.edu.

Notes

The authors declare no competing financial interest.

REFERENCES

(1) Nagl, S.; Wolfbeis, O. S. *Analyst* **2007**, *132*, 507−511.
(2) Pickup, J. C.; Hussain, F.; Evans, N. D.; Rolinski, O. J.; Birch, D. J. S. *Biosens. Bioelectron.* **2005**, *20*, 2555−2565.

(3) Nagl, S.; Stich, M. I. J.; Schaferling, M.; Wolfbeis, O. S. *Anal. Bioanal. Chem.* **2009**, *393*, 1199−1207.
(4) Borisov, S. M.; Wolfbeis, O. S. *Chem. Rev.* **2008**, *108*, 423−461.
(5) Weigl, B. H.; Holobar, A.; Trettnak, W.; Klimant, I.; Kraus, H.; Oleary, P.; Wolfbeis, O. S. *J. Biotechnol.* **1994**, *32*, 127−138.
(6) Rosso, L.; Fernicola, V. C. *Rev. Sci. Instrum.* **2006**, *77*, 034901.
(7) McGraw, C. M.; Khalil, G.; Callis, J. B. *J. Phys. Chem. C* **2008**, *112*, 8079−8084.
(8) Gratton, E. *J. Biomed. Opt.* **2003**, *8*, 381.
(9) Digris, A. V.; Novikov, E. G.; Apanasovich, V. V. *Opt. Commun.* **2005**, *252*, 29−38.
(10) Coolen, R. B.; Papadakis, N.; Avery, J.; Enke, C. G.; Dye, J. L. *Anal. Chem.* **1975**, *47*, 1649−1655.
(11) Peterson, N. C.; Siskos, P. A.; Karayannis, M. I. *Analyst* **1987**, *112*, 821−824.
(12) Sharrock, M. *Rev. Sci. Instrum.* **1977**, *48*, 1202−1206.
(13) Woods, R. J.; Scypinski, S.; Love, L. J. C. *Anal. Chem.* **1984**, *56*, 1395−1400.
(14) Ballew, R. M.; Demas, J. N. *Anal. Chim. Acta* **1991**, *245*, 121−127.
(15) Ballew, R. M.; Demas, J. N. *Anal. Chem.* **1989**, *61*, 30−33.
(16) Waters, P. D.; Burns, D. H. *Appl. Spectrosc.* **1993**, *47*, 111−115.
(17) Sharman, K. K.; Periasamy, A.; Ashworth, H.; Demas, J. N. *Anal. Chem.* **1999**, *71*, 947−952.
(18) Chan, S. P.; Fuller, Z. J.; Demas, J. N.; DeGraff, B. A. *Anal. Chem.* **2001**, *73*, 4486−4490.
(19) Moore, C.; Chan, S. P.; Demas, J. N.; DeGraff, B. A. *Appl. Spectrosc.* **2004**, *58*, 603−607.
(20) Soper, S. A.; Legendre, B. L. *Appl. Spectrosc.* **1994**, *48*, 400−405.
(21) Tellinghuisen, J.; Wilkerson, C. W. *Anal. Chem.* **1993**, *65*, 1240−1246.
(22) Collier, B. B.; McShane, M. J. In *IEEE Sensors 2011*, IEEE: Limerick, Ireland, October 28−31, 2011.
(23) Collier, B. B.; Singh, S.; McShane, M. *Analyst* **2011**, *136*, 962−967.